TÜBİTAK

Turkish Journal of Mathematics

http://journals.tubitak.gov.tr/math/

Research Article

Turk J Math
(2022) 46: 728 – 745

doi:10.3906/mat-2102-76

Elliptical kinematics of the accretive surface growth

Zehra ÖZDEMİR[1,*], **Gül TUĞ**[2]

[1]Department of Mathematics, Arts and Science Faculty, Amasya University, Amasya, Turkey
[2]Department of Mathematics, Faculty of Science, Karadeniz Technical University, Trabzon, Turkey

Received: 15.02.2021 • **Accepted/Published Online:** 04.01.2022 • **Final Version:** 11.03.2022

Abstract: The stresses within the soft tissue are not constant for some shell surfaces. They vary with position along the mantle edge. In this paper, we show that elliptical geometry is more convenient to describe this type of surface. Thus, we introduce the elliptical kinematics along an initial curve and construct some accretive surfaces with an elliptical cross-section. In fact, these surfaces are not only curves with an elliptical cross-sectional curve, but also the material points of the surface follow an elliptical trajectory during their formation. This situation can be easily explained through elliptical motion and elliptical quaternion algebra. Then, we investigate the relationship between velocity and eccentricity of the surfaces and compare it to the case of circular motion. Furthermore, we visualize some examples to support the theoretical results through the MAPLE program.

Key words: Biomathematics, biological growth, Euclidean geometries, special curves, accretive growth, elliptical motions

1. Introduction

Every natural growth or motion pattern inevitably follows one or more geometric shapes. From DNA molecules to our spiral galaxy, many things can be explained with geometric codes. There are endlessly different structures in nature including turtles, snails, seashells, etc. The growth of such structures takes place by adding mass at the boundary of the structure. During this process, various structures are formed with more than one patterning and it usually causes self-similar complex constructions. However, the complexity of these forms makes it difficult to geometrically model them. As B. Mandelbrot says "Clouds are not spheres, mountains are not cones, coastlines are not circles, and bark is not smooth, nor does lightning travel in a straight line". Therefore, the way to construct a mathematically and physically elegant model is to choose an appropriate geometry while investigating the growth of objects.

The first attempts to understand the biological structures mathematically begin with Moseley whose study describes the mathematical aspects of the molluscan shell in terms of elegance and beauty [11]. Then, much of the initial work is done by focusing on the shape of the shells and understanding the evolution of the shell form undergrowth process [2, 6, 8, 16, 17]. However, there was no complete understanding of how the molluscan grows mathematically. Then, Davis mathematically formulated this problem in the complex space [3]. After then, Illert gives an elegant, logical and physically meaningful formulation for the investigation of sea shells growth using such complex coordinates [9]. In [10], the author formulates the seashells in real space

*zehra.ozdemir@amasya.edu.tr

2010 *AMS Mathematics Subject Classification:* MSC: 92B05, 51B20, 14H45, 57R25.

E^3 and obtains equations which can be used for computer simulations. Later, Moulton et al. developed an appropriate mathematical framework and it is not bounded by computer algorithms to generate surfaces [12]. Then, in [19], the authors consider a space curve instead of a planar curve and they use alternative moving frame $\{N, C, W\}$ on the initial curve. This frame ideally describes the growth in the direction of the Darboux vector. In [20], it is investigated that the time dimension in the method effects the growth of the surfaces. Thus, they introduce the model of the growth function in three-dimensional Minkowski space with a timelike or a spacelike generating curve.

The elliptical, circular or commarginal cross-section of a shell, effects its growth velocity. For instance, among the coiled shells of mollusks with nearly circular or elliptical shell margin, ammonites have the slowest expanding. In [4], authors modelled the mechanics of commarginal rib formation via elliptical geometry. They also demonstrated that there is a strong effect of the curvature on the ribbing pattern that manifests in the shell expansion. In three-dimensional spaces, a rotation can be described as only four numbers such that the norm of the quaternion is equal to 1, i.e. a unit quaternion. Quaternions were introduced by Hamilton [7]. Then, Shoemake described the rotation by using the quaternions [18]. Then, in [15], the authors described the elliptical motions through the elliptical quaternions. Quaternions have various applications in computer programs, computer graphics, video games, robotic systems, navigation systems, etc. In mathematics, various surfaces can be constructed by using the quaternions [1, 5]. Some physical law can be described via quaternions [13, 14]. The elliptical motion on an ellipsoid is an important concept since planets usually have ellipsoidal shapes and elliptical orbits, some plants, creatures in nature, some tissues in our body have (elliptical) ellipsoidal shapes and elliptical cross-section. We generate accretive surfaces which have elliptical cross-sections using the elliptical motion and elliptical quaternion algebra in the current work. We provide analytical solutions of the differential equation system obtained by using the elliptical metric and elliptical rotation matrix. Also, we illustrated several examples of the accretive surfaces which can be considered to be more realistic models of the growth processes of some shell species. Furthermore, we demonstrate that the eccentricity of the initial curve strongly effects both the shell expansion rate and energy along the shell margin.

2. Basic concepts and notions

The real vector space $\mathbb{R}^3$ furnished with a positive definite, symmetric bilinear form defined as

$$B : \mathbb{R}^3 \times \mathbb{R}^3 \to \mathbb{R};\ B(\mathbf{u}, \mathbf{v}) = a_1 x_1 y_1 + a_2 x_2 y_2 + a_3 x_3 y_3,$$

which is called $B-$inner product or elliptical inner product, is represented by $\mathbb{R}^3_{a_1,a_2,a_3}$ or $\mathbb{R}^3_B$, where $\mathbf{u} = (u_1, u_2, u_3)$, $\mathbf{v} = (v_1, v_2, v_3) \in \mathbb{R}^3$ and $a_1, a_2, a_3 \in \mathbb{R}^+$. B can be written as $B(\mathbf{u}, \mathbf{v}) = \mathbf{u}^t \Omega \mathbf{v}$, where the associated matrix is

$$\Omega = \begin{bmatrix} a_1 & 0 & 0 \\ 0 & a_2 & 0 \\ 0 & 0 & a_3 \end{bmatrix}.$$

The length of any $\mathbf{u}$ in $\mathbb{R}^3_{a_1,a_2,a_3}$ is given by

$$\|\mathbf{u}\|_B = \sqrt{B(\mathbf{u}, \mathbf{u})}.$$

In $\mathbb{R}^3_{a_1,a_2,a_3}$, any two vectors $\mathbf{u}$ and $\mathbf{v}$ are called elliptically orthogonal if and only if $B(u,v)=0$. The angle between two vectors $\mathbf{u}\neq 0$ and $\mathbf{v}\neq 0$ is defined as

$$\cos\theta=\frac{B(u,v)}{\|\mathbf{u}\|_B\,\|\mathbf{v}\|_B},$$

where θ is compatible with the parameters of the angular parametric equations of an ellipse or elliptical 2-sphere [15].

The elliptical cross product of two vectors in $\mathbb{R}^3_{a_1,a_2,a_3}$ is given by

$$\mathbf{u}\times_E\mathbf{v}=\Delta\begin{vmatrix}\frac{e_1}{a_1} & \frac{e_2}{a_2} & \frac{e_3}{a_3}\\ u_1 & u_2 & u_3\\ v_1 & v_2 & v_3\end{vmatrix}, \tag{2.1}$$

where $\Delta=\sqrt{a_1a_2a_3}$, $a_1,a_2,a_3\in\mathbb{R}^+$ [15]. In Euclidean 3-space $\mathbb{E}^3$, rotations occur on the sphere $x^2+y^2+z^2=r^2$ and a rotation matrix rotates a point or a rigid body through a circular angle about an axis. Thus, the motion actualizes on a circle. In the scalar space $\mathbb{R}^3_{a_1,a_2,a_3}$, rotations occur on the ellipsoid $a_1x^2+a_2y^2+a_3z^2=r^2$ and a rotation matrix rotates a point or a rigid body through an elliptical angle about an axis. Therefore, elliptical rotation is the motion of a point on an ellipse through some angle about a vector (see in Figure 1), [15].

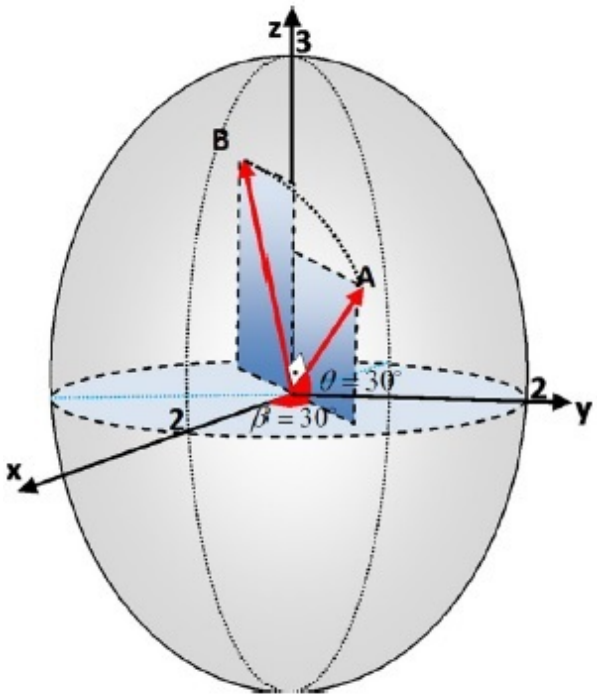

Figure 1. An example for elliptical rotation, [15].

Theorem 2.1 *Let T be a skew symmetric matrix in the following form*

$$T = \Delta \begin{pmatrix} 0 & -\frac{\sqrt{a_2}}{\sqrt{a_1}} \\ \frac{\sqrt{a_1}}{\sqrt{a_2}} & 0 \end{pmatrix}$$

such that the equality $T^t\Omega = -\Omega T$ is satisfied. Then, the matrix exponential

$$R_\theta^{B,u} = e^{T\theta} = I + \sin\theta T + (1-\cos\theta)T^2$$

gives an elliptical rotation on the ellipse $a_1x^2 + a_2y^2 = A,\ a_i, A \in \mathbb{R}^+,\ i \in \{1,2\}$. Furthermore, the matrix $R_\theta^{B,u}$ can be expressed as:

$$\begin{pmatrix} \cos\theta & -\frac{\sqrt{a_2}}{\sqrt{a_1}}\sin\theta \\ \frac{\sqrt{a_1}}{\sqrt{a_2}}\sin\theta & \cos\theta \end{pmatrix},$$

where θ is the elliptical rotation angle [15].

The set of elliptical quaternions is an associative, noncommutative division ring with the basic elements $\{1,i,j,k\}$ and it will be denoted by $\mathbb{H}_E(a_1,a_2,a_3)$:

$$\mathbb{H}_E(a_1,a_2,a_3) = \{q : q = q_0 + q_1i + q_2j + q_3k, q_i \in R,\ i^2 = -a_1, j^2 = -a_2, k^2 = -a_3,\ i = 0,1,2,3\}.$$

The quaternion product of the elliptical quaternions $p_0 + p_1i + p_2j + p_3k$ and $q_0 + q_1i + q_2j + q_3k$ related to the elliptical inner product $(.)$ and the elliptical cross product $\times$ is given by

$$p \otimes q = p_0q_0 - (V_p.V_q) + p_0V_q + q_0V_p + V_p \times V_q. \tag{2.2}$$

The matrix representation of the quaternion product is given by

$$p \otimes q = \begin{bmatrix} p_0 & -a_1p_1 & -a_2p_2 & -a_3p_3 \\ p_1 & p_0 & -p_3\frac{\Delta}{a_1} & p_2\frac{\Delta}{a_1} \\ p_2 & p_3\frac{\Delta}{a_2} & p_0 & -p_1\frac{\Delta}{a_2} \\ p_3 & -p_2\frac{\Delta}{a_3} & p_1\frac{\Delta}{a_3} & b_0 \end{bmatrix} \begin{bmatrix} q_0 \\ q_1 \\ q_2 \\ q_3 \end{bmatrix}. \tag{2.3}$$

Let $q = q_0 + q_1i + q_2j + q_3k$ be a quaternion. The conjugate $\bar{q}$ of the quaternion q is analogues to complex number; that is, $\bar{q} = q_0 - q_1i - q_2j - q_3k$. Then the norm of q is defined as

$$N_q = \sqrt{q\bar{q}} = \sqrt{\bar{q}q} = \sqrt{q_0^2 + a_1q_1^2 + a_2q_2^2 + a_3q_3^2}.$$

For a nonzero quaternion q, its inverse is given as $q^{-1} = \frac{\bar{q}}{N_q^2}$. Also, each quaternion $q = q_0 + q_1i + q_2j + q_3k$ can be written in the form

$$q = N_q(\cos\varphi + \omega_0\sin\varphi), \tag{2.4}$$

where $\cos\varphi = \frac{q_0}{N_q}$, $\sin\varphi = \frac{\sqrt{a_1q_1^2+a_2q_2^2+a_3q_3^2}}{N_q}$, $\omega_0 = \frac{(q_1,q_2,q_3)}{\sqrt{a_1q_1^2+a_2q_2^2+a_3q_3^2}}$, and $\|\omega_0\| = 1$, [15].

The set of the unit elliptical quaternions gives rotations in $\mathbb{R}^3_{a_1,a_2,a_3}$. Thus, the quaternion equation $q = \cos\varphi + \omega_0\sin\varphi$ produces an elliptical rotation matrix M_φ^q by the angle 2φ about the axis ε_0 on the ellipsoid $\mathbb{S}^2_{a_1,a_2,a_3}$, [15].

Theorem 2.2 *Let $q = q_0 + q_1 i + q_2 j + q_3 k = \cos\varphi + \omega_0 \sin\varphi$ be a unit quaternion in $\mathbb{R}^3_{a_1,a_2,a_3}$ then q defines a linear map $F : \mathbb{R}^3 \to \mathbb{R}^3$, defined by $F_\varphi(x) = qxq^{-1}$, where $x \in \mathbb{R}^3$. F generates a rotation about the axis ω_0 and through the angle 2φ. Since F is a linear map, it defines a matrix defined as*

$$M^a_\varphi = \begin{bmatrix} q_0^2 + a_1 q_1^2 - a_2 q_2^2 - a_3 q_3^2 & 2a_2 q_1 q_2 - 2\frac{\Delta}{a_1} q_0 q_3 & 2a_3 q_1 q_3 + 2\frac{\Delta}{a_1} q_0 q_2 \\ 2a_1 q_1 q_2 + 2\frac{\Delta}{a_2} q_0 q_3 & q_0^2 - a_1 q_1^2 + a_2 q_2^2 - a_3 q_3^2 & 2a_3 q_2 q_3 - 2\frac{\Delta}{a_2} q_0 q_1 \\ 2a_1 q_1 q_3 - 2\frac{\Delta}{a_3} q_0 q_2 & 2a_2 q_2 q_3 + 2\frac{\Delta}{a_3} q_0 q_1 & q_0^2 - a_1 q_1^2 - a_2 q_2^2 + a_3 q_3^2 \end{bmatrix}, \tag{2.5}$$

for the ellipsoid, $a_1 x^2 + a_2 y^2 + a_3 z^2 = 1$, [15].

Definition 2.3 *Let us consider that two spaces M (moving) and M^* (fixed), then the one-parameter elliptical homothetic motion of a body defined by*

$$F : M \to M^*; X \to \varsigma U X + T = Y,$$

where U is an elliptical orthogonal matrix, ς is a homothetic scalar, and T is a translation vector.

3. Elliptical accretive growth model

Let us take an initial curve $\psi_0(s) : [0, L] \to \mathbb{R}^3_{a_1,a_2,a_3}$, where s is the material parameter at the time $t = 0$ and we denote $\psi_0(s) := \psi(s, 0)$. The accretive surface growth is formed by the evolution of the curve $\psi(s, 0)$ through the vector field $\upsilon(s, t)$. The vector field $\upsilon(s, t)$ is called the growth velocity of the material point s at time t. The growth velocity leads to the evolution of the initial curve and generates a surface $\psi(s, t)$. The $t-$parameter curves $r(s_0, t)$ corresponds to the cell tracks determined with a fixed initial material point s_0 [12].

Proposition 3.1 *Let $\psi(s, 0)$ be a curve in $\mathbb{R}^3_{a_1,a_2,a_3}$ and $D = (\mathbf{d_1}, \mathbf{d_2}, \mathbf{d_3})$ be an orthonormal frame along this curve and*

$$U = \Delta \begin{bmatrix} 0 & -u_3/a_1 & u_2/a_1 \\ u_3/a_2 & 0 & -u_1/a_2 \\ -u_2/a_3 & u_1/a_3 & 0 \end{bmatrix}, W = \Delta \begin{bmatrix} 0 & -w_3/a_1 & w_2/a_1 \\ w_3/a_2 & 0 & -w_1/a_2 \\ -w_2/a_3 & w_1/a_3 & 0 \end{bmatrix} \tag{3.1}$$

be two skew-symmetric matrices in $\mathbb{R}^3_{a_1,a_2,a_3}$, where $\Delta = \sqrt{a_1 a_2 a_3}$. These matrices called as the elliptical Darboux matrices. Then the components of the matrices U and W satisfy the following nonlinear first order partial differential equations for a given growth velocity υ:

$$\frac{\partial_S \upsilon_1}{\Delta} + u_2 \upsilon_3 - u_3 \upsilon_2 = \xi w_2, \tag{3.2}$$

$$\frac{\partial_S \upsilon_2}{\Delta} + u_3 \upsilon_1 - u_1 \upsilon_3 = -\xi w_1, \tag{3.3}$$

$$\frac{\partial_S \upsilon_3}{\Delta} + u_1 \upsilon_2 - u_2 \upsilon_1 = \frac{\partial_t \xi}{\Delta}, \tag{3.4}$$

$$\frac{\partial_t u_1 - \partial_s w_1}{\Delta} = u_2 w_3 - u_3 w_2, \tag{3.5}$$

$$\frac{\partial_t u_2 - \partial_s w_2}{\Delta} = u_3 w_1 - u_1 w_3, \tag{3.6}$$

$$\frac{\partial_t u_3 - \partial_s w_3}{\Delta} = u_1 w_2 - u_2 w_1, \tag{3.7}$$

where $\xi = (0, 0, \xi)$ *is the stretch factor.*

Proof Let $D = (\mathbf{d_1}, \mathbf{d_2}, \mathbf{d_3})$ be an orthonormal frame along the curve $\psi(s, 0)$. The unit tangent vector defined by

$$\nabla_s^* \psi(s,t) = Dv = \xi \mathbf{d_3}, \tag{3.8}$$

where $Dv = a_1 v_1 \mathbf{d_1} + a_2 v_2 \mathbf{d_2} + a_3 v_3 \mathbf{d_3}$ represents the elliptical product for $v \in \mathbb{R}^3_{a_1,a_2,a_3}$.
The derivations of the frame for the parameters s and t can be given as,

$$\nabla_s^* D = DU, \tag{3.9}$$

$$\nabla_t^* D = DW, \tag{3.10}$$

where ∇^* is the elliptical connection on $\mathbb{R}^3_{a_1,a_2,a_3}$ defined as $\nabla_w^* x_i = \frac{1}{a_i} \partial_w x_i, U$ and W are elliptical Darboux matrices. They are skew-symmetric elliptical orthogonal matrices in $\mathbb{R}^3_{a_1,a_2,a_3}$, that is $D^t \Omega D = \Omega$. The matrix U describes the rotation of the local basis at a fixed point t. The matrix W characterizes the angular velocity of the local basis at a fixed point s.

Attach a general frame $\{\mathbf{d_1}, \mathbf{d_2}, \mathbf{d_3}\}$ to the initial curve at every point. The basis $\{\mathbf{d_1}, \mathbf{d_2}\}$ is determined by elliptical rotation with the angle φ between the normal vector n and $\mathbf{d_1}$. When $\varphi = 0$, it corresponds to the Frenet frame of the curve. Since the vectors $(\mathbf{d_1}, \mathbf{d_2})$ lie in the normal plane, we have the elliptical rotation along the ellipse $a_1 x^2 + a_2 y^2 = A,\ A, a_1, a_2 \in \mathbb{R}^+$ as follows:

$$\mathbf{d_1} = n \cos\varphi + b \frac{\sqrt{a_2}}{\sqrt{a_1}} \sin\varphi,$$

$$\mathbf{d_2} = -n \frac{\sqrt{a_1}}{\sqrt{a_2}} \sin\varphi + b \cos\varphi.$$

As a consequence of the elliptical rotation, the growth velocity vector $\upsilon(s,t)$ through the initial curve can be defined as:

$$\nabla_t^* r = \upsilon(s,t) = Dq, \tag{3.11}$$

where $\upsilon = (\upsilon_1, \upsilon_2, \upsilon_3)$. By using the differentiability conditions on $\psi(s,t)$ we obtain

$$\nabla_s^*(\nabla_t^* r) = \nabla_t^*(\nabla_s^* r), \tag{3.12}$$

$$\nabla_s^*(\nabla_t^* D) = \nabla_t^*(\nabla_s^* D). \tag{3.13}$$

Substitute Eqs. (3.8) and (3.11) in Eq. (3.12), then we obtain

$$D(Uq + \nabla_s^* q) = D(W\xi + \nabla_t^* \xi).$$

Since the general basis of D is orthonormal (i.e. $D^T \Omega D = \Omega$), we reach the following equation

$$\Omega(Uq + \nabla_s^* q) = \Omega(W\xi + \nabla_t^* \xi). \tag{3.14}$$

Writing Eq. (3.13) in terms of the components gives

$$\begin{bmatrix} a_1 & 0 & 0 \\ 0 & a_2 & 0 \\ 0 & 0 & a_3 \end{bmatrix} (\Delta \begin{bmatrix} 0 & -u_3/a_1 & u_2/a_1 \\ u_3/a_2 & 0 & -u_1/a_2 \\ -u_2/a_3 & u_1/a_3 & 0 \end{bmatrix} \begin{bmatrix} v_1 \\ v_2 \\ v_3 \end{bmatrix} + \begin{bmatrix} \partial_S v_1/a_1 \\ \partial_S v_2/a_2 \\ \partial_S v_3/a_3 \end{bmatrix})$$

$$= \begin{bmatrix} a_1 & 0 & 0 \\ 0 & a_2 & 0 \\ 0 & 0 & a_3 \end{bmatrix} (\Delta \begin{bmatrix} 0 & -w_3/a_1 & w_2/a_1 \\ w_3/a_2 & 0 & -w_1/a_2 \\ -w_2/a_3 & w_1/a_3 & 0 \end{bmatrix} \begin{bmatrix} 0 \\ 0 \\ \xi \end{bmatrix} + \begin{bmatrix} 0 \\ 0 \\ \partial_t \xi/a_3 \end{bmatrix}).$$

Then, Equations (3.2–3.4) are obtained. On the other hand, if we write Eqs.(3.9) and (3.10) in Eq.(3.13) we have

$$D(UW + \nabla_s^* W) = D(WU + \nabla_t^* U).$$

Then, we reach the following equation

$$\Omega(UW + \nabla_s^* W) = \Omega(WU + \nabla_t^* U). \tag{3.15}$$

If Eq. (3.15) is rewritten in terms of the components, we get

$$\begin{bmatrix} a_1 & 0 & 0 \\ 0 & a_2 & 0 \\ 0 & 0 & a_3 \end{bmatrix} (\Delta \begin{bmatrix} 0 & -u_3/a_1 & u_2/a_1 \\ u_3/a_2 & 0 & -u_1/a_2 \\ -u_2/a_3 & u_1/a_3 & 0 \end{bmatrix} \Delta \begin{bmatrix} 0 & -w_3/a_1 & w_2/a_1 \\ w_3/a_2 & 0 & -w_1/a_2 \\ -w_2/a_3 & w_1/a_3 & 0 \end{bmatrix}) \tag{3.16}$$

$$+ \begin{bmatrix} a_1 & 0 & 0 \\ 0 & a_2 & 0 \\ 0 & 0 & a_3 \end{bmatrix} \Delta \begin{bmatrix} 0 & -\partial_S w_3/a_1 a_3 & \partial_S w_2/a_1 a_2 \\ \partial_S w_3/a_2 a_3 & 0 & -\partial_S w_1/a_2 a_1 \\ -\partial_S w_2/a_3 a_2 & \partial_S w_1/a_3 a_1 & 0 \end{bmatrix}$$

$$= \begin{bmatrix} a_1 & 0 & 0 \\ 0 & a_2 & 0 \\ 0 & 0 & a_3 \end{bmatrix} (\Delta \begin{bmatrix} 0 & -w_3/a_1 & w_2/a_1 \\ w_3/a_2 & 0 & -w_1/a_2 \\ -w_2/a_3 & w_1/a_3 & 0 \end{bmatrix} \Delta \begin{bmatrix} 0 & -u_3/a_1 & u_2/a_1 \\ u_3/a_2 & 0 & -u_1/a_2 \\ -u_2/a_3 & u_1/a_3 & 0 \end{bmatrix})$$

$$+ \begin{bmatrix} a_1 & 0 & 0 \\ 0 & a_2 & 0 \\ 0 & 0 & a_3 \end{bmatrix} \Delta \begin{bmatrix} 0 & -\partial_t u_3/a_1 a_3 & \partial_t u_2/a_1 a_2 \\ \partial_t u_3/a_2 a_3 & 0 & -\partial_t u_1/a_2 a_1 \\ -\partial_t u_2/a_3 a_2 & \partial_t u_1/a_3 a_1 & 0 \end{bmatrix}.$$

Then, Eq. (3.16) gives us Equations (3.5–3.7). □

Thus, the elliptical accretive surfaces are obtained by integrating the equation $\nabla_s^* \psi(s,t) = Dv$.

Proposition 3.2 *Let $\psi(s,0)$ be a curve in $\mathbb{R}^3_{a_1,a_2,a_3}$ and $D = (\mathbf{d_1}, \mathbf{d_2}, \mathbf{d_3})$ be the Frenet frame along this curve. Then, the elliptical Frenet frame formulas obtained as follows:*

$$\begin{bmatrix} \partial_S \mathbf{d_1} \\ \partial_S \mathbf{d_2} \\ \partial_S \mathbf{d_3} \end{bmatrix} = \begin{bmatrix} 0 & -\tau & \kappa \\ \tau & 0 & 0 \\ -\kappa & 0 & 0 \end{bmatrix} \begin{bmatrix} \mathbf{d_1} \\ \mathbf{d_2} \\ \mathbf{d_3} \end{bmatrix}, \tag{3.17}$$

where $\kappa = B(\partial_s \mathbf{d_3}, \mathbf{d_1})$ and $\tau = B(\partial_s \mathbf{d_1}, \mathbf{d_2})$.

Proof Suppose $D = (\mathbf{d_1}, \mathbf{d_2}, \mathbf{d_3})$ be the Frenet frame along the curve $\psi(s,0)$ and U be a skew-symmetric matrix in $\mathbb{R}^3_{a_1,a_2,a_3}$. Then, we have $\nabla_s^* D^t = U D^t$. This implies,

$$\nabla_S^* \begin{bmatrix} \mathbf{d_1} \\ \mathbf{d_2} \\ \mathbf{d_3} \end{bmatrix} = \Delta \begin{bmatrix} 0 & -u_3/a_1 & u_2/a_1 \\ u_3/a_2 & 0 & -u_1/a_2 \\ -u_2/a_3 & u_1/a_3 & 0 \end{bmatrix} \begin{bmatrix} \mathbf{d_1} \\ \mathbf{d_2} \\ \mathbf{d_3} \end{bmatrix}. \tag{3.18}$$

Then, we deduce

$$\begin{bmatrix} \partial_s \mathbf{d_1} \frac{1}{a_1} \\ \partial_s \mathbf{d_2} \frac{1}{a_2} \\ \partial_s \mathbf{d_3} \frac{1}{a_3} \end{bmatrix} = \Delta \begin{bmatrix} 0 & -u_3/a_1 & u_2/a_1 \\ u_3/a_2 & 0 & -u_1/a_2 \\ -u_2/a_3 & u_1/a_3 & 0 \end{bmatrix} \begin{bmatrix} \mathbf{d_1} \\ \mathbf{d_2} \\ \mathbf{d_3} \end{bmatrix}. \tag{3.19}$$

This gives

$$\begin{bmatrix} \partial_s \mathbf{d_1} \\ \partial_s \mathbf{d_2} \\ \partial_s \mathbf{d_3} \end{bmatrix} = \Delta \begin{bmatrix} 0 & -u_3 & u_2 \\ u_3 & 0 & -u_1 \\ -u_2 & u_1 & 0 \end{bmatrix} \begin{bmatrix} \mathbf{d_1} \\ \mathbf{d_2} \\ \mathbf{d_3} \end{bmatrix}. \tag{3.20}$$

To attach adapted frame, if we choose $\Delta u_2 = \kappa = B(\partial_s \mathbf{d_3}, \mathbf{d_1})$ an $\Delta u_3 = \tau = B(\partial_s \mathbf{d_1}, \mathbf{d_2})$, and $u_1 = 0$, we calculate

$$\begin{bmatrix} \partial_s \mathbf{d_1} \\ \partial_s \mathbf{d_2} \\ \partial_s \mathbf{d_3} \end{bmatrix} = \begin{bmatrix} 0 & -\tau & \kappa \\ \tau & 0 & 0 \\ -\kappa & 0 & 0 \end{bmatrix} \begin{bmatrix} \mathbf{d_1} \\ \mathbf{d_2} \\ \mathbf{d_3} \end{bmatrix}. \tag{3.21}$$

□

Next, we determine the growth velocity components in case of growing in-plane and out-of-plane.

Theorem 3.3 *Let $\psi(s,0)$ be a unit speed arbitrary planar curve with the elliptical frame $\{\mathbf{d_1}, \mathbf{d_2}, \mathbf{d_3}\}$ and the shape variables be $u_1 = u_3 = 0,\ u_2 = \xi\kappa(s,0)$. Then, the form of the growth velocity components is:*

$$v_1 = c_1\beta_1 + c_2\beta_3 + \alpha_1, \tag{3.22}$$

$$v_3 = c_1\beta_3 - c_2\beta_1 + \alpha_3, \tag{3.23}$$

to keep the shape of the curve constant in the plane where it lies. Here $\partial_s\beta_1 = -\Delta u_2\beta_3$, $\partial_s\beta_3 = \xi + \Delta u_2\beta_1$, $\partial_s\alpha_1 = -\Delta u_2\alpha_3$, $\partial_s\alpha_3 = \Delta u_2\alpha_1$, $c_1 = \frac{\partial_t(\xi)}{\xi}$, $c_2 = w_2(t)$, and $\Delta = \sqrt{a_1a_2a_3}$.

Proof Let $\psi(s,0)$ be an arbitrary planar curve which is parameterized by arc-length. For the generate surfaces whose generating curve keeps its shape constant, we take $\|\partial_s r\| = \xi\sqrt{1-(\partial_t\xi)^2}$ and $\kappa(s,t) = \frac{1}{\xi}\kappa(s,0)$, here $\kappa(s,0)$ is the initial curvature. By using the Frenet frame and the shape variables $u_1 = u_3 = 0,\ u_2 = \xi\kappa(s,0)$, we calculate the following second order nonlinear differential equation

$$\partial_s^2 v_1 + \Delta\partial_s u_2 v_3 + \Delta^2 u_2^2 v_1 + \Delta u_2 \partial_t\xi - \partial_s\xi w_2 = 0. \tag{3.24}$$

The solution of this equation provides the accretive surfaces whose generating curve keeps its shape constant in-plane. Now, we find the general solution of Eq. (3.24). The growth velocity can be written in the following form

$$v = c_1(t)\psi + c_2(t)\psi^{\perp} + a(t),$$

where the first, second, and third terms represent dilation, rotation, and a rigid translation, respectively. We can write them as a combination of the frame vectors as follows:

$$\psi = \beta_1\mathbf{d_1} + \beta_3\mathbf{d_3},\ \psi^{\perp} = \beta_3\mathbf{d_1} - \beta_1\mathbf{d_3},\ a = \alpha_1\mathbf{d_1} + \alpha_3\mathbf{d_3}, \tag{3.25}$$

where $\beta_i = B(\psi, \mathbf{d_i}),\ \alpha_i = B(a, \mathbf{d_i})$. Therefore, the components of the growth velocity are written as follows:

$$v_1 = c_1\beta_1 + c_2\beta_3 + \alpha_1, v_3 = c_1\beta_3 - c_2\beta_1 + \alpha_3. \tag{3.26}$$

Then using the Frenet equations, we have

$$\partial_S \mathbf{d_1} = -\Delta u_2 \mathbf{d_3}, \quad \partial_S \mathbf{d_3} = \Delta u_2 \mathbf{d_1}, \tag{3.27}$$

$$\partial_s \beta_1 = -\Delta u_2 \beta_3, \quad \partial_s \beta_3 = \xi + \Delta u_2 \beta_1, \tag{3.28}$$

and

$$\partial_s \alpha_1 = -\Delta u_2 \alpha_3, \quad \partial_s \alpha_3 = \Delta u_2 \alpha_1. \tag{3.29}$$

Considering Equations (3.25)–(3.29) with Eq. (3.24), we obtain

$$c_1 = \frac{\partial_t \xi}{\xi}, c_2 = w_2(t).$$

This relationship gives a rule for the local in-plane velocity components to keep the shape of the generating curve constant. □

Following theorem gives the growth velocity component υ_2 for the accretive surfaces which have elliptical cross-section.

Theorem 3.4 *Let $\psi(s,0)$ be a unit speed circle(ellipse) in $\mathbb{R}^3_{a_1,a_2,a_3}$ with the elliptical frame $\{\mathbf{d_1}, \mathbf{d_2}, \mathbf{d_3}\}$ and the shape variables be $u_1 = u_3 = 0$, $u_2 = \xi$. The shape of the curve does not change if out-of-plane velocity components are written in the following form*

$$\upsilon_2 = \frac{\sigma_1(t)}{\Delta} + \frac{\sigma_2(t)}{\Delta}\cos \Delta s + \frac{\sigma_3(t)}{\Delta}\sin \Delta s, \tag{3.30}$$

where σ_i, $i = \{1,2,3\}$ are arbitrary smooth functions.

Proof Without loss of generality, let the initial ellipse $\psi(s,0)$ have the parametric representation $\psi(s,0) = (\frac{\cos s}{\sqrt{a_1}}, \frac{\sin s}{\sqrt{a_2}}, 0)$. The accretive surface generated by $\psi(s,0)$ can be written by

$$\psi(s,t) = \mathbf{p}(t) - \eta(s,t)\vec{\Phi} \pm \mu(s,t)\vec{\Psi}, \tag{3.31}$$

where $\mathbf{p}(t)$ is a regular unit speed curve and $\vec{\Phi}, \vec{\Psi}$ satisfy

$$\vec{\Phi} = \widetilde{\mathbf{d_3}} \text{ and } \vec{\Psi} = \frac{\cos s}{\sqrt{a_1}}\widetilde{\mathbf{d_1}} + \frac{\sin s}{\sqrt{a_2}}\widetilde{\mathbf{d_2}}. \tag{3.32}$$

In Eq. (3.31), the quantities $\eta(t,s)$ and $\mu(t,s)$ have the form

$$\eta(t,s) = \xi\partial_t\xi, \ \mu(t,s) = \xi\sqrt{1-(\partial_t\xi)^2}. \tag{3.33}$$

Using Equations (3.2)–(3.7), we get

$$\partial_s \upsilon_2 = -\Delta\xi w_1, \tag{3.34}$$

$$\partial_s w_1 = -\Delta u_2 w_3, \tag{3.35}$$

$$\partial_s w_3 = \Delta u_2 w_1. \tag{3.36}$$

Taking two times derivative of Eq. (3.34) and using Eqs. (3.35) and (3.36), we reach the following third order nonlinear differential equation

$$\partial_s^{(3)}\upsilon_2 - (2\frac{\partial_s\xi}{\xi} + \frac{\partial_s u_2}{u_2})\partial_s^2\upsilon_2 + (\Delta^2 u_2^2 + 2\frac{(\partial_s\xi)^2}{\xi^2} - \frac{\partial_s^2\xi}{\xi} + \frac{\partial_s u_2\partial_s\xi}{u_2\xi}) = 0. \tag{3.37}$$

The general solution of Eq. (3.37) gives Equation (3.30). □

In the following theorem, we consider an arbitrary generating curve which is called dressing curve to create a surface via the elliptical motion. For this, we calculate the components of the growth velocity for an arbitrary curve.

Theorem 3.5 *Let* $\mathbf{p}(t)$ *be a unit speed regular curve (dressing curve) attached with a an orthonormal frame* $\widetilde{\mathbf{d}_i}$, $i = 1, 2, 3$, *such that* $\widetilde{\mathbf{d_3}}$ *is tangent to* $\mathbf{p}(t)$ *and it lies the plane perpendicular to* $\widetilde{\mathbf{d_3}}$. *Then, the shape of the curve does not change if the components of the growth velocity are written in the following form:*

$$\begin{aligned}
\upsilon_1 &= \frac{(-\mu\kappa^* \mp \mu\psi_2\tau^* \pm \psi_1\partial_t\mu)(\partial_s^2\psi_1) + (\pm\psi_2\partial_t\mu \pm \mu\psi_1\tau^*)(\partial_s^2\psi_2)}{\sqrt{a_1(\partial_s^2\psi_1)^2 + a_2(\partial_s^2\psi_2)^2}}, \\
\upsilon_2 &= \frac{(1 - \partial_t\eta \mp \mu\psi_1\kappa^*)((\partial_s\psi_1)(\partial_s^2\psi_2) - (\partial_s\psi_2)(\partial_s^2\psi_1))}{\sqrt{a_1(\partial_s^2\psi_1)^2 + a_2(\partial_s^2\psi_2)^2}}, \\
\upsilon_3 &= \frac{(-\mu\kappa^* \mp \mu\psi_2\tau^* \pm \psi_1\partial_t\mu)(\partial_s\psi_1) + (\pm\psi_2\partial_t\mu \pm \mu\psi_1\tau^*)(\partial_s\psi_2)}{\sqrt{a_1(\partial_s^2\psi_1)^2 + a_2(\partial_s^2\psi_2)^2}},
\end{aligned} \tag{3.38}$$

where $\eta(t,s) = \xi\partial_t\xi$, $\mu(t,s) = \xi\sqrt{1-(\partial_t\xi)^2}$, *and* ξ *is the stretch function.*

Proof Consider an arbitrary unit speed curve $\psi(s,0) = (\psi_1(s,0), \psi_2(s,0))$ with the Frenet apparatus $\{\mathbf{d_1}, \mathbf{d_2}, \mathbf{d_3}, \kappa, \tau\}$ and a unit speed curve $\mathbf{p}(t)$ with the Frenet apparatus $\{\widetilde{\mathbf{d_1}}, \widetilde{\mathbf{d_2}}, \widetilde{\mathbf{d_3}}, \kappa^*, \tau^*\}$. To generate a surface we take the dressing curve in the plane of $\widetilde{\mathbf{d_1}}$ and $\widetilde{\mathbf{d_2}}$. In this case, the dressing curve may be written,

$$\psi(s) = \psi_1\widetilde{\mathbf{d_1}} + \psi_2\widetilde{\mathbf{d_2}},$$

at any time t. Then the surface can be written as

$$\psi(s,t) = \mathbf{p}(t) - \eta(s,t)\vec{\Phi} \pm \mu(s,t)\vec{\Psi}, \tag{3.39}$$

where $\eta(t,s) = \xi\partial_t\xi$, $\mu(t,s) = \xi\sqrt{1-(\partial_t\xi)^2}$ with the scaling ξ, and $\vec{\Phi}, \vec{\Psi}$ satisfy

$$\vec{\Phi} = \widetilde{\mathbf{d_3}} \text{ and } \vec{\Psi} = \psi_1\widetilde{\mathbf{d_1}} + \psi_2\widetilde{\mathbf{d_2}}. \tag{3.40}$$

On the other hand, we can calculate the growth velocity field as

$$\partial_t\psi = \upsilon_1\mathbf{d_1} + \upsilon_2\mathbf{d_2} + \upsilon_3\mathbf{d_3}, \tag{3.41}$$

where $\mathbf{d}_i$, $i = 1, 2, 3$ are the local basis for the dressing curve $\psi(s,0)$. Then the growth velocity components are:

$$\begin{aligned}
\upsilon_1 &= B(\partial_t\psi, \mathbf{d_1}), \\
\upsilon_2 &= B(\partial_t\psi, \mathbf{d_2}), \\
\upsilon_3 &= B(\partial_t\psi, \mathbf{d_3}).
\end{aligned} \tag{3.42}$$

Using the Frenet frame $\widetilde{\mathbf{d_i}}$, $i=1,2,3$ on the curve $\mathbf{p}(t)$ and $\partial_t \mathbf{p} = \widetilde{\mathbf{d_3}}$, we have,

$$\begin{aligned} \partial_t \widetilde{\mathbf{d_1}} &= -\kappa^* \widetilde{\mathbf{d_3}} + \tau^* \widetilde{\mathbf{d_2}}, \\ \partial_t \widetilde{\mathbf{d_2}} &= -\tau^* \widetilde{\mathbf{d_1}}, \\ \partial_t \widetilde{\mathbf{d_3}} &= \kappa^* \widetilde{\mathbf{d_1}}. \end{aligned} \tag{3.43}$$

Derivative of Eq. (3.17) with respect to t gives

$$\partial_t \psi(s,t) = (-\mu\kappa^* \mp \mu\psi_2\tau^* \pm \psi_1 \partial_t \mu)\widetilde{\mathbf{d_1}} + (\pm\psi_2 \partial_t \mu \pm \mu\psi_1\tau^*)\widetilde{\mathbf{d_2}} + (1 - \partial_t \eta \mp \mu\psi_1\kappa^*)\widetilde{\mathbf{d_3}}. \tag{3.44}$$

On the other hand, the Frenet frame of the unit speed dressing curve defined via the director vectors as,

$$\begin{aligned} \mathbf{d_1} &= \frac{\partial_s \mathbf{d_3}}{\|\partial_s \mathbf{d_3}\|_B} = \frac{(\partial_s^2 \psi_1)\widetilde{\mathbf{d_1}} + (\partial_s^2 \psi_2)\widetilde{\mathbf{d_2}}}{\sqrt{a_1(\partial_s^2 \psi_1)^2 + a_2(\partial_s^2 \psi_2)^2}}, \\ \mathbf{d_2} &= \mathbf{d_3} \times_E \mathbf{d_1} = \frac{((\partial_s \psi_1)(\partial_s^2 \psi_2) - (\partial_s \psi_2)(\partial_s^2 \psi_1))\widetilde{\mathbf{d_3}}}{\sqrt{a_1(\partial_s^2 \psi_1)^2 + a_2(\partial_s^2 \psi_2)^2}}, \\ \mathbf{d_3} &= \frac{\partial_s \psi}{\|\partial_s \psi\|_B} = (\partial_s \psi_1)\widetilde{\mathbf{d_1}} + (\partial_s \psi_2)\widetilde{\mathbf{d_2}}. \end{aligned} \tag{3.45}$$

By substituting $\mathbf{d_1}$, $\mathbf{d_2}$ and $\mathbf{d_3}$ in Eq. (3.20) we obtain

$$\begin{aligned} \upsilon_1 &= \frac{(-\mu\kappa^* \mp \mu\psi_2\tau^* \pm \psi_1 \partial_t \mu)(\partial_s^2 \psi_1) + (\pm\psi_2 \partial_t \mu \pm \mu\psi_1\tau^*)(\partial_s^2 \psi_2)}{\sqrt{a_1(\partial_s^2 \psi_1)^2 + a_2(\partial_s^2 \psi_2)^2}}, \\ \upsilon_2 &= \frac{(1 - \partial_t \eta \mp \mu\psi_1\kappa^*)((\partial_s \psi_1)(\partial_s^2 \psi_2) - (\partial_s \psi_2)(\partial_s^2 \psi_1))}{\sqrt{a_1(\partial_s^2 \psi_1)^2 + a_2(\partial_s^2 \psi_2)^2}}, \\ \upsilon_3 &= \frac{(-\mu\kappa^* \mp \mu\psi_2\tau^* \pm \psi_1 \partial_t \mu)(\partial_s \psi_1) + (\pm\psi_2 \partial_t \mu \pm \mu\psi_1\tau^*)(\partial_s \psi_2)}{\sqrt{a_1(\partial_s^2 \psi_1)^2 + a_2(\partial_s^2 \psi_2)^2}}. \end{aligned} \tag{3.46}$$

□

4. Elliptical accretive growth model based on elliptical quaternion algebra

For the unit quaternion $q = \cos\psi + \omega_0 \sin\psi = q_0 + q_1 i + q_2 j + q_3 k$, it is an evolution that axis is pure elliptical quaternion $\omega_0 = \frac{(q_1,q_2,q_3)}{\sqrt{a_1 q_1^2 + a_2 q_2^2 + a_3 q_3^2}}$. Namely, an ellipse effectively rotates around the pure quaternion $\omega_0 = \frac{(q_1,q_2,q_3)}{\sqrt{a_1 q_1^2 + a_2 q_2^2 + a_3 q_3^2}}$ with respect to elliptical coordinate systems. Therefore, this elliptical motion produces accretive surfaces that have elliptical cross-sections.

Theorem 4.1 *Let $\mathbf{p} : I \subset \mathbb{R} \to \mathbb{R}^3_{a_1,a_2,a_3}$ be an arc-length parameterized curve with the elliptical Frenet frame apparatus $\{\widetilde{\mathbf{d_1}}, \widetilde{\mathbf{d_2}}, \widetilde{\mathbf{d_3}}, \kappa^*, \tau^*\}$. By using the elliptical quaternion $q(s,t) = \cos s + \widetilde{\mathbf{d_3}}(t)\sin s$, we obtain the parametric equation of the elliptical accretive surfaces $\psi(s,t)$, which are scaling with nonconstant function $\xi(s,t)$, are given via the unit elliptical quaternion $q(s,t) \otimes \widetilde{\mathbf{d_1}}(t)$ in the following parametric form:*

$$\psi(s,t) = \mathbf{p}(t) - \eta(s,t)\widetilde{\mathbf{d_3}}(t) + \mu(s,t) \otimes q(s,t) \otimes \widetilde{\mathbf{d_1}}(t),$$

where $\eta(t,s)=\xi\partial_t\xi,\ \mu(t,s)=\xi\sqrt{1-(\partial_t\xi)^2}$ *with the scaling* ξ, *and* R_t^q *is the matrix form of the unit elliptical quaternion* $q(s,t)$.

Proof Assume that $\psi(s,t)$ be a quaternionic accretive surface generated by the curve $\mathbf{p}(t)$. Then, we have

$$\psi(s,t)=\mathbf{p}(t)-\eta(s)\widetilde{\mathbf{d_3}}(t)\pm\mu(s)(\cos s)\widetilde{\mathbf{d_1}}(t)+\sin s\widetilde{\mathbf{d_2}}(t)).$$

If we use the elliptical quaternion product for unit quaternion $q(s,t)=\cos s+\widetilde{\mathbf{d_3}}(t)\sin s$ and the pure quaternion $\widetilde{\mathbf{d_1}}(t)$, we obtain

$$q(s,t)\otimes\widetilde{\mathbf{d_1}}(t)=\widetilde{\mathbf{d_1}}(t)\cos s+\widetilde{\mathbf{d_2}}(t)\sin s.$$

Then using the last equation, we reach the following form of the quaternionic (ECS)

$$\psi(s,t)=\mathbf{p}(t)-\eta(s,t)\widetilde{\mathbf{d_3}}(t)\pm\mu(s,t)q(s,t)\otimes\widetilde{\mathbf{d_1}}(t)$$

and the matrix representation of the surface given as

$$\psi(s,t)=\mathbf{p}(t)-\eta(s,t)\widetilde{\mathbf{d_3}}(t)\pm\mu(s,t)R_\theta^q\widetilde{\mathbf{d_1}}(t).$$

□

Corollary 4.2 *The formation through an elliptical motion of an accretive surface* $\psi(s,t)$ *can be described by an elliptical homothetic motion and the parametric form of via the homothetic motion is given as follows:*

$$\psi(s,t)=\mathbf{p}(t)-\eta(s,t)\widetilde{\mathbf{d_3}}(t)\pm\mu(s,t)R_t^q\widetilde{\mathbf{d_1}}(t).$$

Proof If we choose the translation vector and homothetic scalar of the elliptical homothetic motion, respectively, as $\beta(t):=\mathbf{p}(t)-\eta(s,t)\widetilde{\mathbf{d_3}}(t),\ \mu(s,t)$. Since R_t^q is an elliptical orthogonal matrix, we can say that $\psi(s,t)=\beta(t)+\mu(s,t)R_t^q\widetilde{\mathbf{d_1}}(t)$ is the elliptical homothetic motion. □

Corollary 4.3 *Let* $\mathbf{p}:I\subset\mathbb{R}\to\mathbb{R}^3_{a_1,a_2,a_3}$ *be an arc-length parameterized curve with the elliptical Frenet frame apparatus* $\{\widetilde{\mathbf{d_1}},\widetilde{\mathbf{d_2}},\widetilde{\mathbf{d_3}},\kappa,\tau\}$. *By using the elliptical quaternion* $q(s,t)=\cos s+\widetilde{\mathbf{d_3}}(t)\sin s$, *we obtain the parametric equation of the elliptical accretive surfaces* $\psi(s,t)$, *which are scaling with constant function* $\xi(s,t)=r$, *are given via the unit elliptical quaternion* $q(s,t)\otimes\widetilde{\mathbf{d_1}}(t)$ *in the following parametric form:*

$$\psi(s,t)=\mathbf{p}(t)+rq(s,t)\otimes\widetilde{\mathbf{d_1}}(t),$$

where r *is an arbitrary constant.*

Corollary 4.4 *Let* $\mathbf{p}:I\subset\mathbb{R}\to\mathbb{R}^3_{a_1,a_2,a_3}$ *be an arc-length parameterized curve with the elliptical Frenet frame apparatus* $\{\widetilde{\mathbf{d_1}},\widetilde{\mathbf{d_2}},\widetilde{\mathbf{d_3}},\kappa^*,\tau^*\}$. *By using the elliptical quaternion* $q(s,t)=\cos s+\widetilde{\mathbf{d_3}}(t)\sin s$, *we obtain the parametric equation of the elliptical accretive surfaces* $\psi(s,t)$, *which are scaling with constant function* $\xi(s,t)=r(s)$, *are given via the unit elliptical quaternion* $q(s,t)\otimes\widetilde{\mathbf{d_1}}(t)$ *in the following parametric form:*

$$\psi(s,t)=\mathbf{p}(t)+r(s)q(s,t)\otimes\widetilde{\mathbf{d_1}}(t).$$

5. Some motivated examples

First we generate surfaces that have an arbitrary cross-section curve with elliptical shell margin by using the elliptical motion. If we take $\upsilon_1 = -c, \upsilon_2 = \frac{\sigma_1}{\Delta} + \frac{\sigma_2}{\Delta}(1 + 0.05 * \cos(s)) \cos \Delta s,\ \upsilon_3 = 0$. Also, the figures can be obtained via the elliptical quaternion $\mathbf{q} = (1 + 0.05 * \cos(s))q$, where $q = \cos s + \widetilde{\mathbf{d_3}}(t) \sin s$ is a unit elliptical quaternion and $\widetilde{\mathbf{d_3}}$ is the tangent vector of the curve $\mathbf{p}(t)$. The images of the surfaces illustrated in Figure 2.

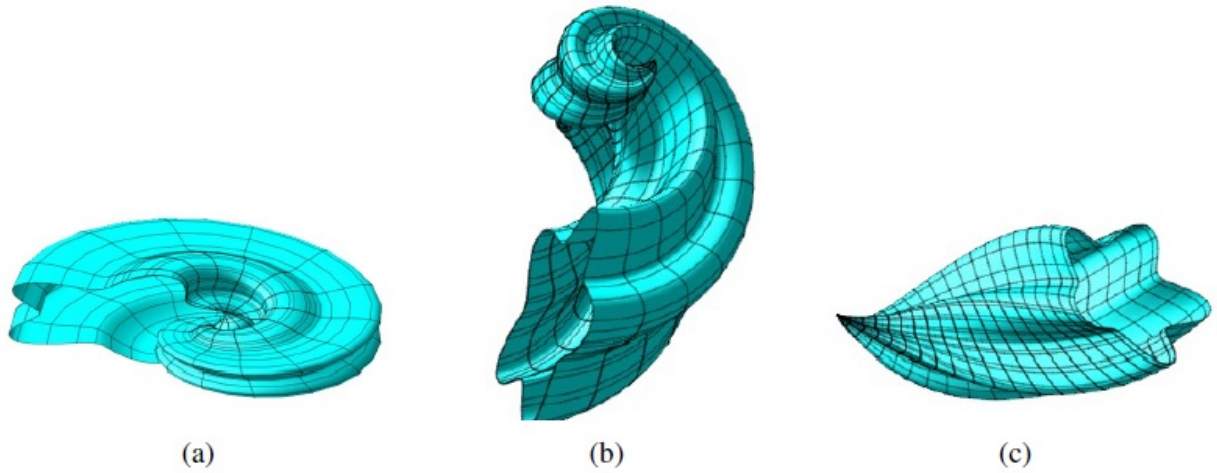

Figure 2. An arbitrary cross-section surfaces obtained by elliptical motion. (a) $a_0 = 1, a_1 = 1, a_2 = 9, a_3 = 4, \sigma_1 = 1, \sigma_2 = 0.5, c = 0.025$, (b) $a_0 = 1, a_1 = 16, a_2 = 2, a_3 = 0.5, \sigma_1 = 1, \sigma_2 = 0.3, c = 0.025$, (c) $a_0 = 1, a_1 = 1, a_2 = 4, a_3 = 9, \sigma_1 = 2, \sigma_2 = 0.8, c = 0.5$.

Next, choosing the initial curve as an ellipse given by $\psi(s, 0) = (\frac{\cos s}{\sqrt{a_1}}, \frac{\sin s}{\sqrt{a_2}}, 0)$ in the following examples to get elliptical cross-sections. Such a choice provides more realistic examples of the accretive surfaces representing some biological structures. The figures can be obtained via the unit elliptical quaternion $q = \cos s + \widetilde{\mathbf{d_3}}(t) \sin s$, where $\widetilde{\mathbf{d_3}}$ is the tangent vector of the curve $\mathbf{p}(t)$.

Let us take the components of the growth velocity as $\upsilon_1 = -c, \upsilon_2 = \frac{\sigma_1}{\Delta} + \frac{\sigma_2}{\Delta} \cos \Delta s,\ \upsilon_3 = 0$. In this kind of growth model, the cell tracks follow an elliptical logarithmic spiral (see Figure 3a). When the binormal growth scales with the stretch factor ξ, i.e. the velocity components are $\upsilon_1 = -c, \upsilon_2 = \xi(\frac{\sigma_1}{\Delta} + \frac{\sigma_2}{\Delta} \cos \Delta s), \upsilon_3 = 0$. Then, we calculate $\xi = 1 + k_1 t$. For this accretive growth form, the cell tracks follow an elliptical algebraic logarithmic spiral. Then, the obtained surfaces are similar to the Nautilus or ammonite shell forms (see Figure 3b). When we take $\upsilon_1 = -c, \upsilon_2 = \frac{\sigma_1}{\Delta} + \frac{\sigma_2}{\Delta} \xi(s, t) \cos \Delta s, \upsilon_3 = 0$, the cell tracks follow an ellipse (see Figure 3c).

If we take the growth velocity components as follows:

$$\upsilon_1 = -c,\ \upsilon_3 = \sigma_3,\ \upsilon_2 = \frac{\sigma_1}{\Delta} + \frac{\sigma_2}{\Delta} \cos(\Delta s). \tag{5.1}$$

Then the initial curve follows an elliptical path out of plane. The images of this form surfaces are plotted in Figures 4 and 5.

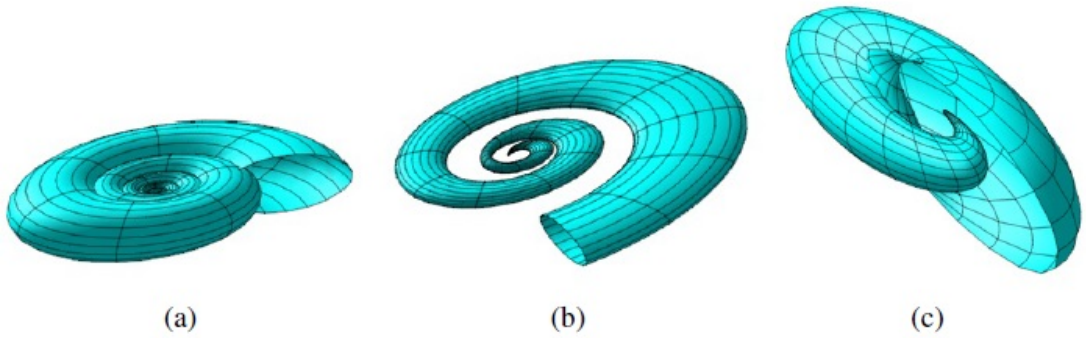

Figure 3. (a) $a_0 = 1, a_1 = 1, a_2 = 9, a_3 = 4, \sigma_1 = 1, \sigma_2 = 0.5, c = 0.025$, (b) $a_0 = 1, a_1 = 2, a_2 = 16, a_3 = 0.5, \sigma_1 = 1, \sigma_2 = 0.3, c = 0.025$, (c) $a_0 = 1, a_1 = 1, a_2 = 4, a_3 = 9, \sigma_1 = 2, \sigma_2 = 0.8, c = 0.5$.

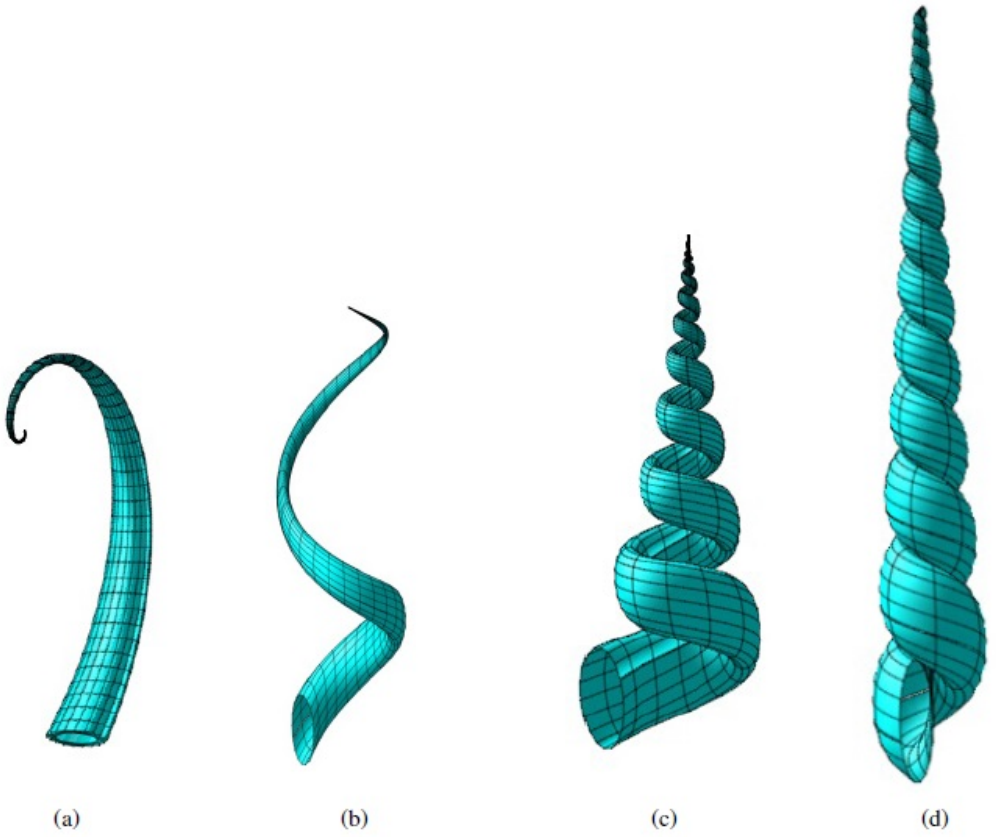

Figure 4. (a) $a_0 = 0.1, a_1 = 4, a_2 = 1, a_3 = 9, \sigma_1 = 1, \sigma_2 = 0.4, c = -0.025$, (b) $a_0 = 0.1, a_1 = 4, a_2 = 1, a_3 = 9, \sigma_1 = 1, \sigma_2 = \sigma_1/a_0, c = -0.025$, (c) $a_0 = 0.1, a_1 = 4, a_2 = 1, a_3 = 9, \sigma_1 = 1, \sigma_2 = t, c = -0.025$, (d) $a_0 = 0.1, a_1 = 4, a_2 = 1, a_3 = 9, \sigma_1 = 1, \sigma_2 = \sigma_1/a_0, c = -0.025$.

Next, if we take the components of the growth velocity as

$$\upsilon_1 = -c,\ \upsilon_3 = 0, \upsilon_2 = \frac{\sigma_1}{\Delta} + \frac{\sigma_2}{\Delta}\cos(\Delta s - \sigma_3 t), \tag{5.2}$$

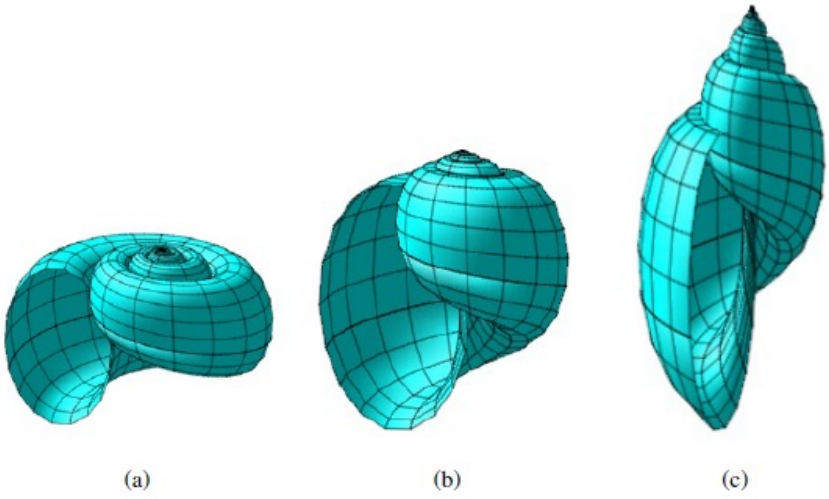

Figure 5. (a) $a_0 = 0.1, a_1 = 20, a_2 = 4, a_3 = 10, \sigma_1 = 0.4, \sigma_2 = 2, c = -0.025$, (b) $a_0 = 0.1, a_1 = 20, a_2 = 4, a_3 = 10, \sigma_1 = 0.2, \sigma_2 = 2, c = -0.025$, (c) $a_0 = 0.1, a_1 = 14, a_2 = 3, a_3 = 9, \sigma_1 = 0.2, \sigma_2 = 2, c = -0.025$.

then the initial curve follows an elliptical path out of plane. In the previous examples, each point of the generating curve follows the planar elliptical trajectories. This form surfaces are illustrated in Figure 6.

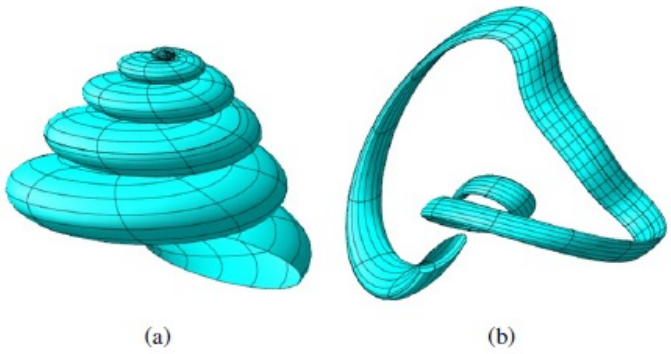

Figure 6. (a) $a_0 = 0.1, a_1 = 4, a_2 = 1, a_3 = 9, \sigma_1 = 1, \sigma_2 = \sigma_1/a_0, c = -0.025$, (b) $a_0 = 0.1, a_1 = 4, a_2 = 2, a_3 = 9, \sigma_1 = 1, \sigma_2 = \sigma_1/a_0, c = -0.025$.

6. Discussions and conclusion

The form in Eq. (3.46) implies a general feature of the accretive growth. By using the elliptical kinematics, we obtain more realistic accretive surfaces. From a global perspective, this relates to the case of the circular growth model. There is, however, a distinction between the two, which although subtle, is biologically relevant. The difference is understood in terms of cell tracks, growth velocity and energy. For the circular growth model, each material point follows a circular trajectory and for the elliptical growth model each material point follows an elliptical trajectory around the growth axis. This implies differences for the growth velocity of the structure. For instance, among the coiled shells of mollusks with nearly circular or elliptical shell margin, ammonites have the slowest expanding. In particular, the growth rate of each material point on a circular generating curve

is faster than the growth rate of each material point on the elliptical generating curve. This idea is, also, investigated by Erlich (see [4]) through the effect of the eccentricity e on ribbing pattern. They discussed the effect of expansion rate on the ribbing pattern at constant eccentricity and effect of the allometric increase in eccentricity. The change to an elliptical geometry means that the stresses within the soft tissue are not constant but rather vary with position along the mantle edge. This added complexity renders a force balance description impractical such as presented in Moulton (see [12]). Therefore, it will be very useful to use elliptical motions and elliptical quaternion algebra for the growth model to be defined in this form of growth model. Thus, the key technique of our study is to use elliptical kinematics and is to use elliptical quaternions. This motion properly describes the accretive growth of the surfaces that have elliptical cross-section. In fact, these surfaces are not only curves with an elliptical cross-sectional curve, but also the material points of the surfaces follow an elliptical trajectory (ellipse, elliptical helix, elliptical spiral, etc.) during their formation. Furthermore, the growth velocity is defined with the help of the eccentricity number e that is a measure of how much it deviates from being circular and given by the equation $e = \sqrt{1 - \frac{a_2}{a_1}}$. If we assume that $a_1 > a_2$, then we can give the reference circle and the related ellipse as in Figure 7.

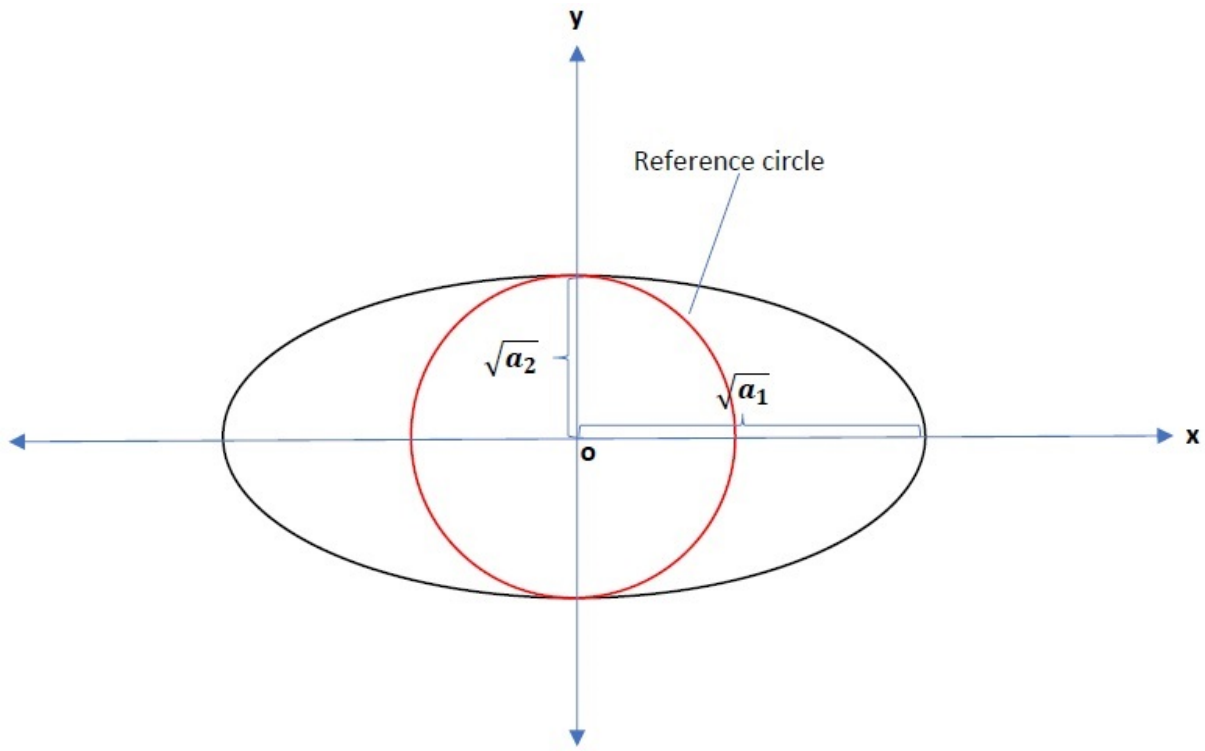

Figure 7. Reference circle and ellipse.

Choosing the generating curve as the curve $\psi(s,0) = (\frac{\cos s}{\sqrt{a_1}}, \frac{\sin s}{\sqrt{a_2}}, 0)$, i.e. the elliptical cross-section. Then we have $u_1 = u_3 = 0$, $u_2 = \xi$, then from equations (3.2)-(3.7), we can calculate that $w_1 = \frac{\sigma_2}{\xi}\sin(\Delta s - \sigma_3 t)$,

$w_2 = h(t),\ w_3 = -\frac{\sigma_2}{\xi}\cos(\Delta s - \sigma_3 t)$. These gives the components of the velocity q computed as follows:

$$\begin{aligned} \upsilon_1 &= c_1\cos(\Delta s - \sigma_3 t) + c_2\sin(\Delta s - \sigma_3 t) + \frac{\partial_t \xi}{\Delta}, \\ \upsilon_2 &= f(t)\frac{\sigma_1}{\Delta} + g(t)\frac{\sigma_2}{\Delta}\cos(\Delta s - \sigma_3 t), \\ \upsilon_3 &= \frac{-c_2\cos(\Delta s - \sigma_3 t) + c_1\sin(\Delta s - \sigma_3 t)}{\xi} + \frac{h(t)}{\Delta}. \end{aligned} \tag{6.1}$$

Now, we specify the velocity field $\upsilon(s,t)$ as follows by choosing $\sigma_3 = 0,\ c_1 = 1, c_2 = 0$, and $f(t) = g(t) = 1$, we calculate the following equations:

$$\begin{aligned} \upsilon_1 &= \cos(\Delta s), \\ \upsilon_2 &= \frac{\sigma_1}{\Delta} + \frac{\sigma_2}{\Delta}\cos(\Delta s), \\ \upsilon_3 &= \sin(\Delta s), \end{aligned}$$

where $\Delta = a_1\sqrt{a_3(1-e(t)^2)}$, $e(t)$ is a constant function $0 < e(t) < 1$.

In Figure 8, we can say that the growth is faster than a reference circle as e approach to 1. However, the growth have the approximately the same speed of the reference circle as e approach to 0. That is, velocity increases with increasing eccentricity number.

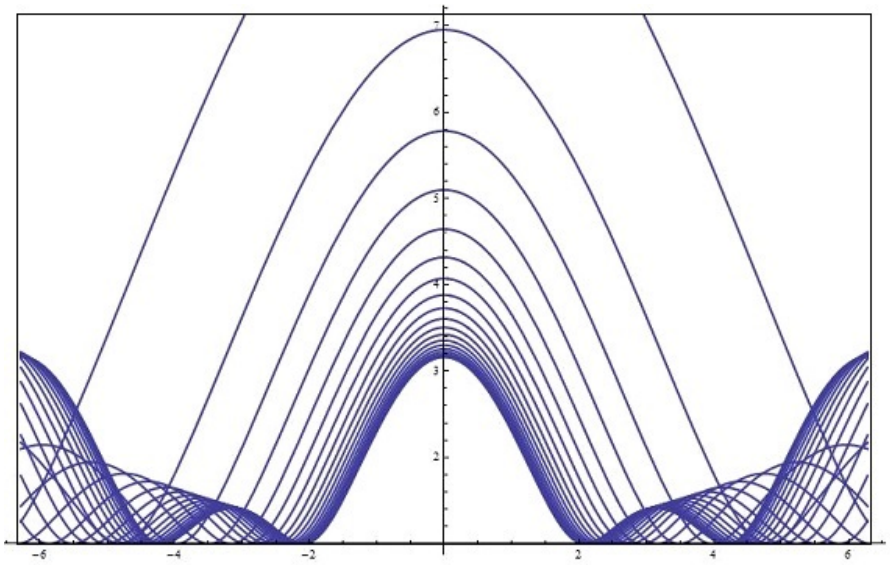

Figure 8. Growth velocity components of material point s at time t. This graphs are plotted according to the increment of e in 0.05 for the intervals $0 < e < 1$, i.e. $e = \{0.05, 0.1, ..., 0.95\}$.

Consequently, the cross-section and path of the material points of the surfaces effect its growth velocity. Undoubtedly, since the growth rate is affected by these factors, the change in the growth energy of the accretive surfaces can be investigated.

References

[1] Aslan S, Yaylı Y. Canal surfaces with quaternions. Advances in Applied Clifford Algebras 2016; 26: 31-38.

[2] Boettiger AN, Oster G. Emergent complexity in simple neural systems. Communicative & Integrative Biology 2009; 2 (6): 467-470.

[3] Davis PJ. The Schwarz Function and its Applications, Carius Monograph 17. Mathematical Association of America, 1974.

[4] Erlich A, Moulton DE, Goriely A, Chirat R. Morphomechanics and Developmental Constraints in the Evolution of Ammonites Shell Form. Journal of Experimental Zoology Part B: Molecular and Developmental Evolution 2016; 326 (7): 437-450.

[5] Gök İ. Quaternionic approach of canal surfaces constructed by some new ideas. Advances in Applied Clifford Algebras 2016, doi:10.1007/s00006-016-0703-9 1408.

[6] Hammer Ø, Bucher H. Models for the morphogenesis of the molluscan shell. An international Journal of Palaentology and Stratigraphy 2005; 38 (2): 111-122.

[7] Hamilton WR. On quaternions; or on a new system of imagniaries in algebra. The London, Edinburgh, and Dublin Philosophical Magazine and Journal of Science 1844; 25 (3): 489-495.

[8] Hans M. The Algorithmic Beauty of Sea Shells. Springer, 2009.

[9] Illert C. Formulation and solution of the classical problem, I Seashell geometry. Nuovo Cimento 1987; 9 (7): 791-814.

[10] Illert C. Formulation and solution of the classical problem, II Tubular three dimensional surfaces. Nuovo Cimento 1989; 11: 761-780.

[11] Moseley H. On the Geometrical Forms of Turbinated and Discoid Shells. Philosophical Transactions of the Royal Society of London 1838; 128: 351-370.

[12] Moulton DE, Goriely A. Surface growth kinematics via local curve evolution. Journal of Mathematical Biology 2014; 68 (1-2): 81-108.

[13] Özdemir Z. A New Calculus for the Treatment of Rytov's Law in the Optical Fiber. Optik - International Journal for Light and Electron Optics 2020; 216: 164892.

[14] Özdemir Z, Cansu G, Yaylı Y. Kinematic modeling of Rytov's law and electromagnetic curves in the optical fiber based on elliptical quaternion algebra. Optik - International Journal for Light and Electron Optics. Doi:https://dx.doi.org/10.1016/j.ijleo.2021.166334.

[15] Özdemir M. An Alternative Approach to Elliptical Motion. Advances in Applied Clifford Algebras 2016; 26: 279-304.

[16] Raup DM, Michelson A. Theoretical Morphology of the Coiled Shell. Science 12, 1965; 147: 1294-1295. doi: 10.1126/science.147.3663.1294.

[17] Raup DM. The Geometry of Coiling in Gastropods. Proceedings of the National Academy of Sciences of the United States of America 1961; 47 (4): 602-609.

[18] Shoemake K. Animating rotation with quaternion curves. In: Proceedings of the 12th Annual Conference on Computer Graphics and Interactive Techniques (SIG-GRAPH '85), vol. 19, pp. 245-254, ACM, New York, NY, USA, 1985.

[19] Tuğ G, Özdemir Z, Gök İ, Ekmekci FN. Accretive Darboux Growth along a Space Curve. Applied Mathematics and Computation 2018; 316: 516524.

[20] Tuğ G, Özdemir Z, Aydın SH, Ekmekci FN. Accretive growth kinematics in Minkowski 3-space. International Journal of Geometric Methods in Modern Physics 2017; 14: 1750069.